Nanoscale Shear and Indentation Measurements in Transcrystalline α-Isotactic Polypropylene

Ella Amitay-Sadovsky,[†] Sidney R. Cohen,[‡] and H. Daniel Wagner*[,†]

Department of Materials & Interfaces, and Chemical Services, The Weizmann Institute of Science, Rehovot 76100, Israel

Received July 11, 2000

ABSTRACT: The relation between the mechanical properties and the lamellar morphology of the α-isotactic polypropylene transcrystalline interphase in a fiber composite was investigated by means of nanometric shear and directional indentation measurements, using scanning force microscopy. Measurements were performed along directions parallel and perpendicular to the transcrystalline growth direction. A key finding is the inversion of the shear modulus anisotropy ratio from 2.3 to 0.5 as the crystal grows away from the fiber. On the basis of this finding, an improved view of the hierarchical lamellar and molecular order of the transcrystalline layer is proposed.

Introduction

The anisotropic mechanical properties of oriented α-isotactic polypropylene (α-iPP) are studied in this work at the nanometric level. The oriented polymer consists of a transcrystalline (TC) region[1] which forms in composite materials when a high-modulus fiber is embedded into an appropriate semicrystalline polymer melt. Upon cooling from the melt and under specific conditions, nucleation starts at the surface of the fiber, which plays the role of a heterogeneous nucleation center. Radial crystal growth normal to the fiber surface takes place, eventually enclosing the fiber.[2−3] The morphology and mechanical behavior of the TC interphase, and its contribution to the mechanical performance of composite materials, have not yet been fully explained.[5−7] Direct measurements aimed at resolving these issues were performed here at the nanometer scale, using nanoshear and nanoindentation techniques.

Previous microindentation[7] and nanoindentation[8] results obtained with α-iPP TC interphases have shown that when indentation is performed with elongated tips (such as a Knoop diamond indenter or a bladelike silicon scanning force microscopy (SFM) tip), the Young's modulus is higher in the direction perpendicular to the TC growth, compared to the modulus parallel to that direction. This result was obtained in experiments performed near the middle of the TC region, i.e., at a distance of about 30 μm from the fiber surface.[8] The observed difference in Young's moduli was quantified by means of the anisotropy ratio, which was found to increase as the size of indentation (the contact area) decreased. This ratio was 1.3 for microindentation tests, compared to values of up to 3 for nanoindentation tests. Such data was interpreted by means of a morphological model in which the *c* axis of the polypropylene chain is perpendicular to the $z-x$ plane of the fiber, where the *z* axis is the fiber axis. This is in contradiction with earlier models.[9−10] On the basis of wide-angle X-ray scattering (WAXS) measurements of α-iPP, Dean et al.[10] suggested a parent/daughter lamellar growth scheme in which the *c*-axis of the parent lamellae lie within the $z-x$ plane parallel to the fiber *z* axis, and the daughter lamellae lie at 80.7° from the parent. It is important to point out that the experiments of Dean et al. were performed with a relatively high (30%) volume fraction of fibers in the composite, which implies that their scheme is presumably valid only for the TC region in close proximity to the fiber. Our previous nanoindentation tests were performed at a larger distance from the fiber surface, which may explain the apparent contradiction between the two models. This contradiction is hypothesized to be due to a change in the lamellar *c* axis direction, vide infra. As a final comment, Norton and Keller found[11] that, as the crystallization temperature increases, the number of daughterlike lamellae decreases, until about 139−140 °C at which no more daughter lamellae are observable. In the present work the crystallization temperature was 139 °C, and therefore, daughterlike lamellae were not expected.

The novelty in the present investigation can be described as follows. Previous studies consisted of morphological examinations of the TC region at distances from the fiber that were not comparable to each other (either close to or away from the fiber surface). Here we systematically investigate the effect of distance from the fiber surface on the mechanical properties of the TC zone, using shear and indentation at the nanometric level, and infer a morphological model based on the mechanical results. An additional feature of the present work was to increase the resolution of the measurements, using ultrasharp SFM tips for shear measurements, such that the contact area was only 2% of the contact area used in our previous study.

Experimental Procedure

The specimen was prepared so that the TC region would be exposed on the external surface, for further mechanical testing. Complete details of the preparation procedure are given elsewhere.[7−8] Crystallization toward the monoclinic α form was carried out at 139 °C, and the resulting thickness of the TC area (on each side of the fiber) was 80 μm on average.

In the following description, axes to which measurement directions are referenced are defined with respect to the TC growth direction, denoted by the symbol g (Figure 1). The TC growth direction is perpendicular to the fiber longitudinal *z* axis. The angle of indentation is the angle between g and the direction of the applied shear force, F_L, in the nanoshear tests,

[†] Department of Materials & Interfaces, The Weizmann Institute of Science.

[‡] Chemical Services, The Weizmann Institute of Science.

10.1021/ma001193d CCC: $20.00
Published on Web 01/26/2001

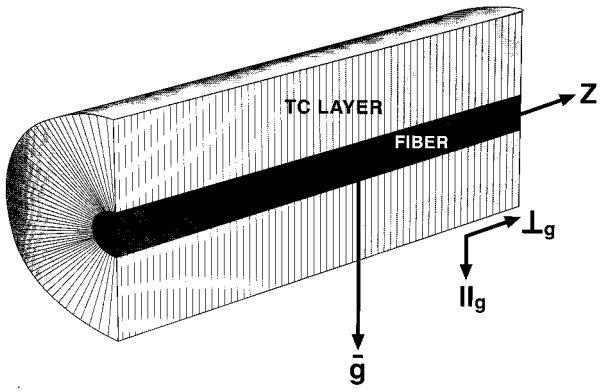

Figure 1. Definition of measurement directions relative to the transcrystalline growth direction (g) in a transcrystalline region around a single fiber.

or between g and the long axis of the indenting bladelike tip, in the nanoindentation tests. The shear (or lateral) and normal forces were applied parallel (||) and perpendicular (⊥) to the TC growth direction g. We denote the measurements parallel to the growth direction as $||_g$ and those perpendicular to the growth direction as $\perp_g$. The forces were applied at distances of 1−2 and ∼30 μm from the fiber surfaces. Shear measurements at ∼60 μm from the fiber were also performed.

Nanoindentation measurements using a bladelike SFM tip were performed as previously.[8] Young's moduli of the TC layer close to the fiber surface (1−2 μm) and away from it (30 μm) were obtained. For these experiments, it was essential to determine the exact profile of the tip over the indentating surface. For this, reverse imaging on sharp spikes (NT-MDT, calibration grid TGT01) was used with the calibration protocol described previously. [8]

For the shear measurements, tip shapes were monitored before the experiments on a sample of random Ti spikes (General Microdevices, Edmonton, Canada). Tips chosen had radii of 10−15 nm, and smooth profile. The contact area was estimated from the radius of contact $a = [R \times D]^{1/2}$ where R is the tip radius as approximated from the measured tip shape and D is the sample deformation (estimated from Herzian theory). No care was taken to further characterize the tip shape since the parameter of interest is the anisotropy ratio in which tip-shape related effects are factored away in the calculations outlined below. Shear measurements were achieved using a specially designed tube scanner within tube scanner arrangement whereby the inner, concentric scanner was used to obtain a lateral dither and the outer one provided the sample movement for imaging. The probes were sharp, approximately conical tips ("Pointbrobes" for contact SFM, Nanosensors GMBH). An image of the TC surface was obtained before applying the lateral force. The lateral displacement was obtained by connecting the x-electrodes of the inner SFM tube scanner to a signal generator, providing a triangular pulse of amplitude corresponding to a lateral displacement of 160 nm. Only single-shot pulses were used, so that each friction loop (Figure 2) represents one back and forth pass of the sample relative to the tip. The trace starts in the lower center of the loop, and proceeds in counterclockwise fashion, as indicated by the numbers: 1−2, onset of motion starting with tip at rest and sticking on the surface; 2−3, sliding in forward direction; 3−4, reversal of sliding direction with sticking; 4−5, sliding in backward direction; 5−6, second reversal of sliding direction, with sticking. Shear is related to the upward slope, after point 3, as outlined in the computation section below.The spike in the middle is an artifact due to on/off characteristics of the single pulse applied.

Three shear measurements were performed within each 1 × 1 μm^2 imaged area. Tests were performed in three to six different TC areas, yielding a total of 9−18 measurements at each distance from the fiber surface. The same was repeated in the perpendicular direction. Testing was repeated with two different tips, and the results are reported in Table 1.

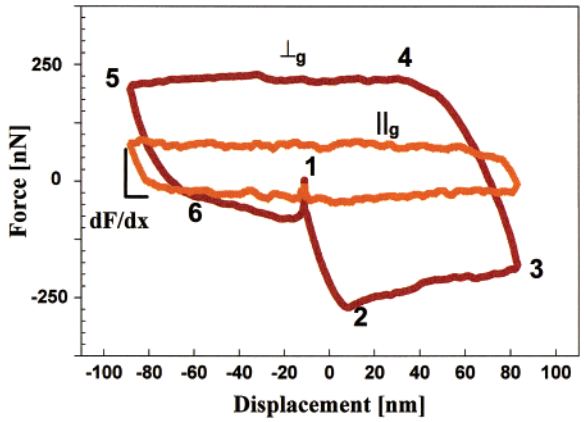

Figure 2. Typical shearing loops as a function of the lateral tip−surface relative displacement in transcrystalline α-iPP measured perpendicular ($\perp_g$) and parallel ($||_g$) to the transcrystalline growth direction at a distance of 1−2 μm from the fiber. The numbers on the curve represent specific points in the single friction loop (see text).

Table 1. Average Shear Moduli of α-iPP Transcrystalline Specimens Measured in Different Orientations as a Function of the Distance from the Fiber Surface

distance from the fiber (μm)	shear modulus ($||_g$) [GPa]	no. of expts	shear modulus ($\perp_g$) [GPa]	no. of expts	anisotropy ratio $G_{\perp_g}/G_{||_g}$
1−2	0.22 ± 0.09	15	0.51 ± 0.0.10	10	2.32
∼30	0.26 ± 0.07	27	0.13 ± 0.04	28	0.50 (1/2.0)
∼60	0.56 ± 0.04	5	0.28 ± 0.05	5	0.50 (1/2.0)

To convert the measured signals to forces, additional calibration and calculations are required.[12] The cantilever's spring constant was calculated from the measured resonance frequency. The sensor response against tip (lateral) displacement was measured using a silicon surface, which was considered as an infinitely hard surface compared to the polymer. The shear modulus was then calculated using the equation[13]

$$G^* = \frac{k_{\text{contact}}\left[\frac{N}{m}\right]}{8a[nm]} \tag{1}$$

where G^* is the relative shear modulus value, a is the radius of contact (estimated to be 10 nm), and

$$k_{\text{contact}} = \left[\frac{dx}{dF} - \frac{1}{k_{\text{lever}[l]}}\right]^{-1} \tag{2}$$

where dx/dF is the slope obtained from the frictional force vs x displacement curves before the onset of sliding (Figure 2). The slope taken was the initial slope of the curve, since contact area can grow with increased lateral motion.[13] This is important for the bigger curves, which show a distinct curvature over the sticking region as can be seen in Figure 2 between points 3 and 4. The cantilever lateral stiffness, $k_{\text{lever}[l]}$, is equal to $(4k_nGL^2)/(3t^2E)$, where k_n, G, L, t, and E are the normal stiffness of the tip (0.35N/m), its shear modulus (60 GPa, from ref 13), its length (440 μm), its height (12 μm), and its Young's modulus (170 GPa), respectively. The actual shear modulus, G_{TC}, of the TC layer was then calculated from a simple rule-of-mixtures expression:

$$G_{TC} = \frac{(2 - \nu_{TC})}{\left(\frac{1}{G^*} - \frac{(2 - \nu_{tip})}{G_{tip}}\right)} \tag{3}$$

where the Poisson ratios of the TC zone and tip are $\nu_{TC} \approx 0.35$ and $\nu_{tip} \approx 0.1$,[8] respectively. The shear modulus of the tip, G_{tip}, is 60 GPa.[8]

The contact areas probed in the present study are of the order of 300 nm^2, compared to the much larger contact areas (10 000−20 000 nm^2) used in our previous study[8] and for the nanoindentations of this study.

Results

Mechanical Properties Adjacent to the Fiber. In Figure 2 we present a set of typical results from nanoscale shear tests performed in the TC area at a very short distance (1−2 μm) from the fiber surface. Shear loops for an experiment performed in the $\perp_g$ direction (thus, perpendicular to the TC growth direction), and for an experiment performed in the $\|_g$ direction (parallel to the growth direction), are presented. The sloped sides of the loops correspond to the sticking regions prior to sliding, whereas the (approximately) horizontal sections of the loop correspond to the sliding regions. It is clear that the maximum shearing force (the height of the loop) required to shear in the $\|_g$ direction is significantly smaller than the maximum shearing force in the $\perp_g$ direction. Further, the shape of the $\perp_g$ curve is asymmetric, with the right part of the curve having larger hysteresis than the left. The calculated shear modulus in the $\|_g$ direction (0.22 GPa) is thus smaller than in the $\perp_g$ direction (0.51 GPa); see Table 1. Third, the shear modulus anisotropy ratio between those directions is found to be 2.32 (Table 1).

Nanoindentation tests were also performed at the same short distance (1 to 2 μm) from the fiber surface, using bladelike SFM tips as in our previous study. These revealed that the Young's modulus in the $\perp_g$ direction is higher (0.40 GPa) than in the $\|_g$ direction (0.28 GPa), resulting in a Young's modulus anisotropy ratio of 1.42. Thus, a similar trend is observed using both techniques, albeit in a milder way, as will be discussed.

Mechanical Properties away from the Fiber. Shearing tests were also performed at distances of 30 and 60 μm away from the fiber. Plots similar to Figure 2 are obtained, but the maximum force required to shear in the $\|_g$ direction is now larger than the force required to shear in the $\perp_g$ direction. This results in high shear moduli (0.26 and 0.56 GPa at 30 and 60 μm from the fiber, respectively) in the $\|_g$ direction, compared to the shear moduli (0.13 and 0.28 GPa) in the $\perp_g$ direction. The resulting shear modulus anisotropy ratios are thus reversed compared to the previous case, yielding a value of 0.50 in both cases (Table 1). In all cases, the variability between the loops within each direction is small. Here, the dependence of the shape of the curves on shear direction is reversed from that seen close to the fiber: fatter curves ($\|_g$) display the same asymmetry seen for the $\perp_g$ curves close to the fiber in Figure 2 whereas the smaller curves ($\perp_g$) are symmetrical.

For the ensuing discussion, it is important to note that from 30 to 60 μm from the fiber, the shear modulus values increase for both the parallel and perpendicular directions (Table 1). Also, the reversal of the anisotropic ratio that occurs between measurements close to the fiber and 30 μm away is due mostly to the drastic change of shear modulus values in the $\perp_g$ direction (the modulus in the $\|_g$ direction remains nearly unchanged), see Table 1. In contrast with the shearing measurements, nanoindentation tests do not result in a reversal of the Young's modulus anisotropic ratio from 1−2 (ratio = 1.42) to 30 μm (ratio = 1.54) from the fiber. The Young's modulus values obtained in our previous study (at 30 μm only) resulted in anisotropic ratios of between 1.6 up to 3, and seemed to strongly depend on the shape (the length-to-width ratio) of the blade tip used. A conjectural conclusion from these statements is that the difference between the two tests is in their resolution. This is further reinforced by the fact that, as indicated earlier, the contact area probed by the tip in a shearing experiment is about 300 nm^2, whereas it is 10 000−20 000 nm^2 in a nanoindentation experiment. The resolution of the shear measurement is thus significantly better than that of the nanoindentation measurements.

Discussion

Two simplified views of hierarchical levels may serve as guides in the discussion, namely, the deck of cards model (at the level of the lamellar assemblies) and the folded wire (springlike) model (at the intralamellar organizational level). Regarding the dimensions, according to Bassett,[14] following crystallization at 140 °C, the α-iPP lamellae thickness is ∼20 nm. Neither its width nor the interlamellar distance are known precisely, although one usually assumes[18] that the width is at most 1 μm (but from this work we suspect that it is probably much less, around 200 nm) and the interlamellar distance is about 20 nm (since the degree of crystallinity was measured by X-ray diffraction to be 50−60% here). The distance between fold stems (a^*) is ∼6 Å.[14]

We now turn to the morphological implications regarding the transcrystalline lamellar assembly, based on the results presented here. The molecular chain direction in a lamella may be parallel either to the fiber z axis (Figure 3a) or to its y axis (Figure 3b). Thus, at the specimen surface under the SFM tip, two options exist for the lamellar ordering: (1) the $a-c$ plane of the lamella is exposed, revealing the thickness (20 nm) of the "card deck"; or (2) the $a-b$ plane of the lamella (thus the plane that contains the lamellar folds) is exposed, revealing the width of the "cards". The width of the lamellae is unknown, as recalled earlier, but we conjecture that it is not as large as in spherulitic iPP (where it is about 1 μm). Indeed, in the case of a TC structure, there is not enough space for each lamella to develop in the width direction, due to the high nucleation density at the surface of high modulus carbon fibers.

Shear Measurements. Let us assume that the TC morphology may be described by the first lamellar arrangement described above and in Figure 3a. Thus, when a shearing force is applied, the SFM tip is running on top of the lamellar $a-c$ planes. Recall that the diameter of the loading tip and the thickness of the lamella are of the same order of magnitude and that, prior to shearing the polymer, the tip is slightly indenting the lamella. The ensuing shearing movement in the lamellar growth direction is resisted by the relatively weaker intermolecular polymer chain bonds (similar to the opening of a spring), whereas the shearing motion perpendicular to the lamellar growth direction (thus, parallel to the fiber) is resisted by stronger covalent bonding along the molecule axis.

If the TC morphology is assumed to be described by the second lamellar arrangement (Figure 3b), the SFM tip is now shearing the $a-b$ plane. The shearing movement in the lamellar growth direction is resisted by forces that are again due to weak intermolecular bonding, whereas the shearing perpendicular to the lamellar growth direction (thus, parallel to the fiber) is

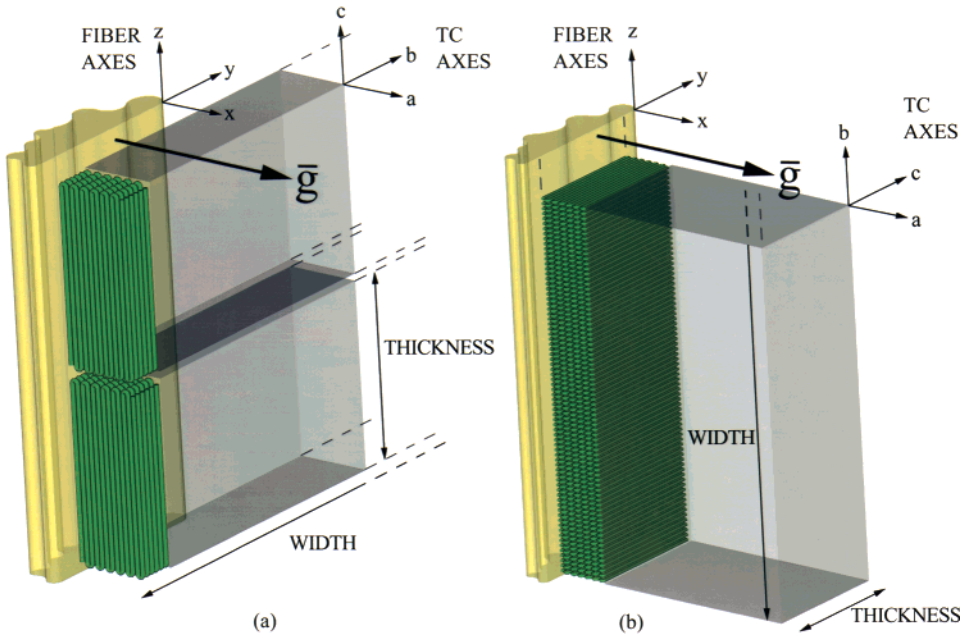

Figure 3. Proposed schematic morphological models of transcrystalline structure in α-iPP. Two extreme cases are illustrated: (a) molecular chain direction parallel to *z* axis of fiber; (b) molecular chain direction parallel to *y* axis of fiber. The lamellar growth direction is indicated as g. The *a*-axis notation of the polymer chain is the *a** usually used in the literature.[10]

now barely resisted because the molecular chains along that direction are less strongly attracted to each other.

The data presented in Table 1 seem better explained by the first lamellar arrangement when shearing is performed in the TC area that is close to the fiber, whereas the second lamellar arrangement provides a better support for the data away from the fiber. Interestingly, this hypothesis could explain the shape of the curves in Figure 2: when the tip is sliding along the length of the polymer chains ($\perp_g$ close to fiber, or $\|_g$ far away) it could stretch and/or orient the chain so that on the ensuing return path, friction is reduced. For this reason, shear was always evaluated on the first pass, not the return one. When the tip slides across the chains ($\|_g$ close to the fiber or $\perp_g$ far away) the close packing of the chains resists any such deformation so that the loop is symmetric.

Indentation Measurements. As already suggested, nanoindentation measurements are somewhat less sensitive to the polymer chain arrangement within the lamellae, due to the width dimensions of the bladelike tip (50−100 nm). At this scale, the indenting tip is only able to sense differences between lamellar assemblies. In the first model, Figure 3a, the exposed lamellar facet is its thickness which, according to Bassett,[14] is ∼20 nm. The SFM image in Figure 4a, taken at 1−2 μm from the fiber surface, reveals 30−50 nm thick elongated features, which might possibly be correlated with the thicknesses of the exposed lamellar facets. In the second model, Figure 3b, the exposed lamellar facet is its width, which is assumed to be of the order of up to ∼1000 nm.[18] However, the (typical) SFM image in Figure 4b, taken at 50−60 μm away from the fiber surface, reveals oval objects with maximal thicknesses of 200 nm which can possibly be correlated with the widths of the exposed lamellar facets. This would make the lamellar width as much as five times thinner than conventionally presumed. A consequence of this is that the nanoindentation experiments, which use a bladelike tip with width of 50−100 nm, significantly larger than tip used for the

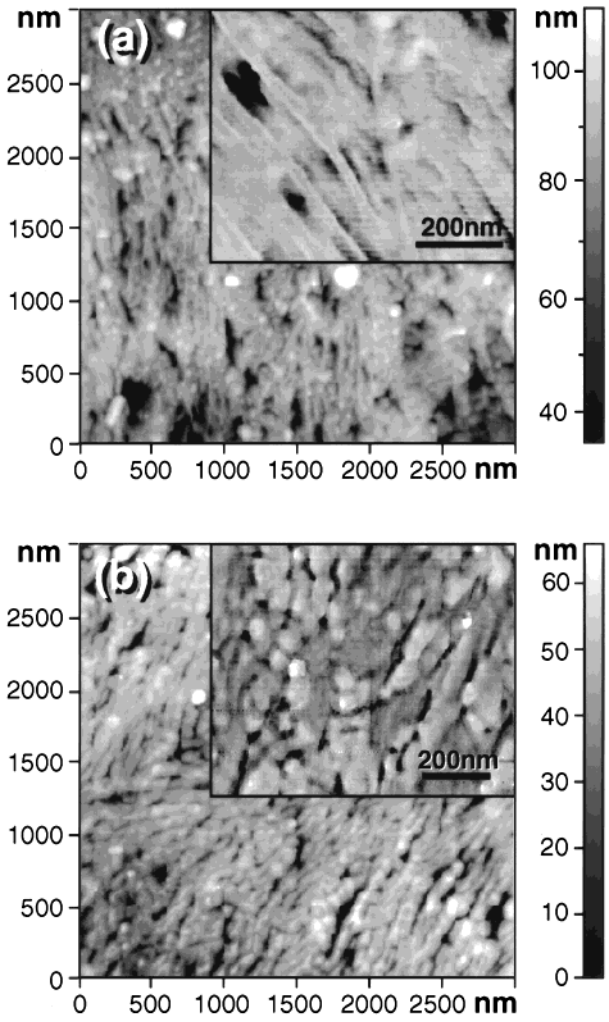

Figure 4. SFM images of transcrystalline α-iPP: (a) 1−2 μm from the fiber surface; (b) 30 μm from the fiber surface. The fiber direction is horizontal.

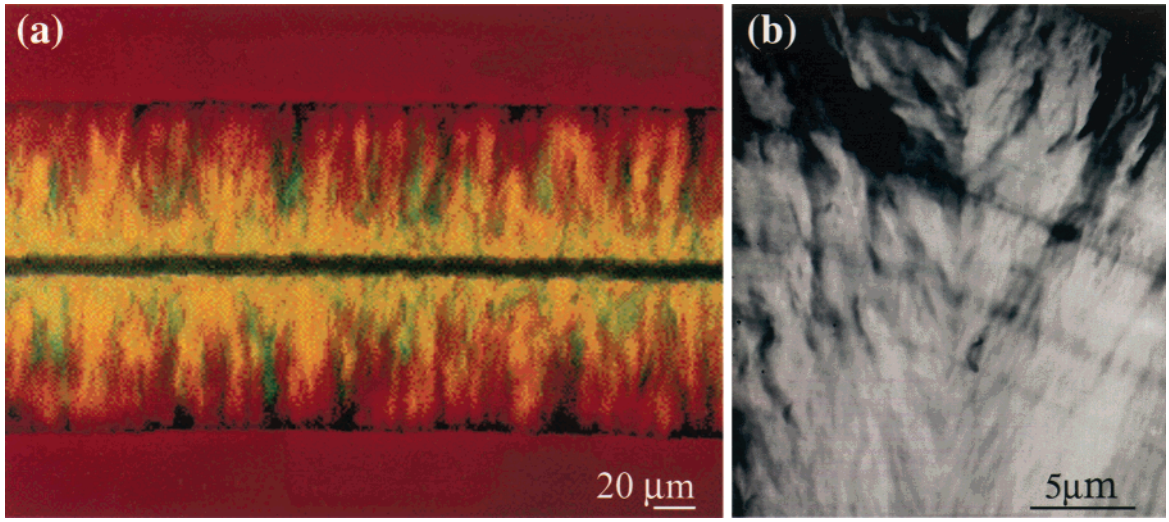

Figure 5. (a) Optical microscope view of transcrystalline α-iPP region around a high modulus carbon fiber. Note the change in birefringence as a function of distance from the fiber. (b) TEM view of transcrystalline α-iPP region, showing an apparent change in morphological features as a function of distance from the fiber surface (the fiber direction is horizontal).

shear experiments, have less resolving power in distinguishing between the morphologies close to and away from the fiber surface (however, the tip still remains sensitive to the orientations of the structures).

Morphological Considerations. A conclusion that arises from the above discussion is that, due to the difference in resolving power between the two experiments (shear and nanoindentation), the actual polymeric entities tested are different under the two tips, since in one case (shear) the internal structure of the lamellae is tested, and in the other (indentation) assemblies of lamellae are probed.

From the shear measurements and the SFM topographical observations performed at different distances from the fiber, and possibly also from optical photographs (Figure 5a) which show a change in birefringence as the TC layer grows away from the fiber surface, we conclude that it is likely that the orientation of the α-iPP transcrystalline lamellar layers progressively varies as a function of the distance from the fiber. This also seems evident from TEM pictures such as in Figure 5b. This change—the cause of which is not clear—is thought to be thermodynamically driven, and is also observed in other polymers such as polyethylene.[15−16] Two situations seem possible, namely a progressive lamellar twist up to a constant configuration, or a lamellar sheafing (which may or may not be accompanied by twisting as well). For illustration purposes a lamellar twist configuration is schematically presented in Figure 6, from which one can envision how a configuration change could lead to a mechanical property variation as a function of distance from the fiber surface. However, the experimental evidence presented so far does not allow us to decide which lamellar growth model is correct. Additional information is necessary and recent synchrotron experiments[17] may shed additional light on this issue. Such a spiraling lamella would grow by twisting about its axis at 1−2 μm from the fiber up to 30 μm away from it. Near the fiber, the TC growth would be epitaxial with the molecular *z*-axis aligned in the fiber *c*-axis direction (Figure 3a), as observed by Dean et al.[10] for relatively high fiber content random composites. Outward, the lamellae progressively twist theoretically up to a maximum that would correspond to the configuration in Figure 3b, although we have no evidence for this.

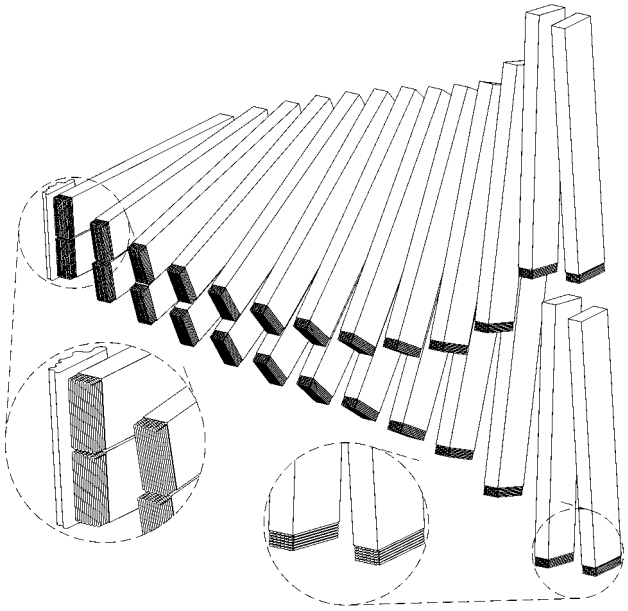

Figure 6. Schematic model of lamellar twisting as a function of distance from a fiber substrate, where the thickness of the lamellae is 20 nm and the width is 200 nm.

It is important to note that the lamellar twisting hypothesis would involve stringent steric effects between neighboring lamellae. Indeed, the rotation of neighboring parallelipipedic entities would necessarily force the "decks" to open up so as to make space for the larger emerging width of all lamellae (Figure 6). It may also be possible to explain the increasing shear modulus value as a function of distance from the fiber (between 30 and 60 μm) on the basis of steric effects involved in the lamellar twisting model, but again more evidence for the validity of twisting is necessary.

Finally, our earlier microindentation and nanoindentation tests[7,8] revealed that extrema in stiffness arise, in fact, at an intermediate angle of ≈30−40° relative to g. This again might reflect local morphological changes linked to twisting or sheafing such as observed in transcrystalline PE.[15−16]

Conclusions

The underlying principle of this study is that it may be possible to extract morphological information from mechanical measurements performed at the nanometric scale. Thus, the mechanical properties of the α-isotactic polypropylene transcrystalline interphase in a fiber composite were investigated by means of nanometric shear and directional indentation measurements, using scanning force microscopy. Measurements were performed along directions parallel and perpendicular to the transcrystalline growth direction. It was found that the shear modulus anisotropy ratio changes from 2.3 to 0.5 as the crystal grows away from the fiber. This inversion of the anisotropy ratio, measured by means of the more sensitive nanoshear tests, reflects a morphological change in the arrangement of lamellae as a function of distance from the fiber. Two options regarding these morphological changes are lamellar twisting and sheafing, but more sensitive measurements are needed to resolve this issue. From the nano mechanical results and from SFM images we conjecture that the lamellar thickness in TC areas is 30−50 nm, similar to that in spherulites. The lamellar width of TC specimens, however, is up to 200 nm, much smaller than in spherulitic polypropylene. Twisting arrays would involve severe steric effects between neighboring lamellae, and the rotation of neighboring parallelipipedic entities would necessarily cause a reorganization of the lamellar "edifice", which in turn would have strong mechanical consequences as measured here.

Acknowledgment. H.D.W. is the recipient of the Livio Norzi Professorial Chair. This project was supported by a grant from the MINERVA Foundation, and by the Israel Ministry of Science. We thank Prof. D. Bassett for informal discussions regarding the lamellar dimensions. The concept that a change in morphology might take place as a function of distance in TC α-PP was first suggested by Prof. Gad Marom and Dr. Eric Assouline. Thanks are due to Dr. Arnold Lustiger for extensive and fruitful discussions.

References and Notes

(1) Keller, A. *J. Polym. Sci.* **1955**, *15*, 31−38.
(2) Hoecker, F.; Karger-Kocsis, J. *Polym. Bull.* **1993**, *31*, 707−714.
(3) Hsiao, B. S.; Chen, E. J. H. *Mater. Res. Soc. Symp. Proc.* **1990**, *170*, 117−121.
(4) Folkes, M. J.; Hardwick, S. T. *J. Mater. Sci.* **1987**, *6*, 656−658.
(5) Huson, M. G.; Mcgill, W. J. *J. Polym. Sci., Part B: Polym. Phys.* **1985**, *23*, 121−128.
(6) Gati, A.; Wagner, H. D. *Macromolecules* **1997**, *30*, 3933−3935.
(7) Amitay-Sadovsky, E.; Wagner, H. D. *J Polym. Sci., Part B: Polym. Phys.* **1999**, *37*, 523−530.
(8) Amitay-Sadovsky, E.; Cohen, S. R.; Wagner, H. D. *Appl. Phys. Lett.* **1999**, *74*, 2966−2968.
(9) Lustiger, A.; Marzinsky, C. N.; Mueller, R. R.; H. D. Wagner, *J. Adhes.* **1995**, *53*, 1−14.
(10) Dean, D. M.; Rebenfeld, L.; Register, R. A.; Hsiao, B. S. *J. Mater. Sci.* **1998**, *33*, 4797−4812.
(11) Norton, R. D.; Keller, A. *Polymer* **1985**, *26*, 704−716.
(12) Wisenhorn, A. L.; Khorsardi, M.; Kasas, S.; Gotzost, V.; Butt, H. *Nanotechnology* **1993**, *4*, 106−113.
(13) Carpick, R. W.; Ogletree, D. F.; Salmeron, M. *Appl. Phys. Lett.* **1997**, *70*, 1548−1550.
(14) White, H. M.; Bassett, D. C. *Polymer* **1997**, *38*, 5515−5520.
(15) Keith, H. D.; Padden, F. J., Jr. *Polymer* **1984**, *25*, 28−32.
(16) Stern, T.; Wachtel, E.; Marom, G. *J. Polym. Sci., Part B: Polym. Phys.* **1997**, *35*, 2429−2433.
(17) Assouline, E.; Wachtel, H.; Grigull, S.; Lustiger, A.; Wagner, H. D.; Marom, G. Submitted for publication.
(18) Bassett, D. C.; Lustiger, A. Private communications.

MA001193D